terize the details of a cycle of another oscillatory reaction.

Some of the above studies could be done easily, while others would require additional apparatus. Any study of a system as complex as this will always leave loose ends and suggest further tests. We believe that the work reported here provides a sufficient extension of understanding to justify publication at this time.

Acknowledgment. This work was supported in part by a grant from the National Science Foundation. After the experimental work had been completed, Professor Stanley D. Furrow of the Berks Campus of The Pennsylvania State University pointed out the Liebhafsky[8] observations that made necessary the dashed extension of the curve in Figure 6.

Dynamics of Protein Domain Coalescence. 2†

Gary P. Zientara, Janice A. Nagy, and Jack H. Freed*

Baker Laboratory, Department of Chemistry, Cornell University, Ithaca, New York 14853 *(Received: July 26, 1981; In Final Form: September 21, 1981)*

Dynamic effects of a model pair correlation function and Oseen's tensor hydrodynamic interactions are included in the study of the kinetics of protein domain coalescence using the numerical approach of Zientara, Nagy, and Freed [*J. Chem. Phys.*, **73**, 5092 (1980)]. Modifications to the previously reported results due to hydrodynamic drag and either Debye–Hückel or Coulombic electrostatic forces are presented. A model domain pair correlation function is also incorporated to more accurately simulate the spatial and energetic aspects of hydrophobic bonding. Applying this extended model, the variation of coalescence lifetimes with ionic strength and temperature is then calculated and discussed with reference to published experimental data. A frequently observed but anomalous temperature variation in a renaturation rate constant is explained by our results.

I. Introduction

An analysis of the kinetics of protein domain coalescence, an elementary step in the complex protein folding process, has previously been introduced by Karplus and Weaver[1] in terms of a diffusion–reaction model. The analytic results of their model for the mean lifetime of uncoalesced domains in the limit of low coalescence probability[1b] (i.e., reactivity) complement the study of Adam and Delbrück,[2] who discussed the mean lifetime of reactive species confined to finite spatial domains in the limit of infinite reactivity. Recently, the first passage time approach of Szabo et al.[3,4] has unified previous theories by consideration of the complete range of reactivities. These studies provide an excellent mathematical basis for the study of protein domain coalescence assuming simple domain interactions. The restriction to simple interactions is due to the analytical mathematical difficulties in solving the Smoluchowski equation with a general interaction potential, $U(r)$.

Model systems of protein dynamics, however, must include protein–solvent, protein–ion, and protein–protein interactions so that model results can be useful in predicting and interpreting experimental data. In order to present a method which allows an unrestricted choice of domain–domain and domain–solvent interactions, Zientara et al.[5] (hereafter referred to as I) have employed numerical solutions of the Smoluchowski equation to calculate the mean lifetime of coalesced domains. The model utilized in I is based upon that of Karplus andd Weaver[1] modified to include the orientation dependence of domain reactivities, interdomain electrostatic forces mediated by a solution with a finite ionic strength, and the effects of domain hydration shells.

In this study we first discuss hydrodynamic effects on the simple Brownian diffusive motion of the protein domains. This modification is included through Oseen's tensor corrections to the diffusion tensor and is applied in the study of domains interacting through Debye–Hückel or Coulombic potentials. Also, the hydration shell structure that provides the energy barrier involved in hydrophobic bonding in protein systems is simulated by employing a model domain–domain pair correlation function within the mathematical framework of I. The ionic strength dependence of the coalescence lifetimes is then described by a Debye–Hückel interaction including hydrodynamic effects. Finally, the variation in the rate of coalescence with temperature is examined for different cases of electrostatic interactions.

The discussion of the theoretical and numerical aspects of the calculations is contained in section II. The general effects upon predicted values of mean coalescence lifetimes of hydrodynamic terms and a pair correlation function are presented in section III. In section IV the ionic strength and temperature dependence of coalescence rates are discussed and compared with experiments. A summary of the results of this study appears in section V.

II. Theory

Hydrodynamics. The calculation of the mean lifetime of uncoalesced protein domains has been developed in I through numerical solutions of the Smoluchowski equation

† Supported by NIH Grant GM-25862 and NSF Grant CHE 80-24124.

(1) (a) M. Karplus and D. L. Weaver, *Nature (London)*, **260**, 404 (1976); (b) M. Karplus and D. L. Weaver, *Biopolymers*, **18**, 1421 (1979); (c) D. L. Weaver, *Biophys. Chem.*, **10**, 245 (1979); (d) D. L. Weaver, *J. Chem. Phys.*, **72**, 3483 (1980).

(2) G. Adam and M. Delbrück, in "Structural Chemistry and Molecular Biology", A. Rich and W. Davidson, Ed., Freeman, San Francisco, 1968.

(3) A. Szabo, K. Schulten, and Z. Schulten, *J. Chem. Phys.*, **72**, 4350 (1980).

(4) The first passage time approach is reviewed by N. S. Goel and N. Richter-Dyn, "Stochastic Models in Biology", Academic Press, New York, 1974.

(5) G. P. Zientara, J. A. Nagy, and J. H. Freed, *J. Chem. Phys.*, **73**, 5092 (1980).

0022-3654/82/2086-0824$01.25/0

with a "sink" or reaction term

$$\frac{\partial P(\mathbf{r},t)}{\partial t} = \nabla_r \cdot \boldsymbol{D} \cdot \left[\nabla_r P(\mathbf{r},t) + \frac{1}{k_B T} P(\mathbf{r},t) \nabla_r U(\mathbf{r}) \right] + K(\mathbf{r}) P(\mathbf{r},t) \quad (1)$$

where $P(\mathbf{r},t)$ is the probability distribution of domain pairs at separation $\mathbf{r}$ at time t influenced by a potential $U(\mathbf{r})$. The spatial dependence of irreversible domain reaction is described through $K(\mathbf{r})$. Complete details of the theoretical treatment can be found in I. The probability distribution of uncoalesced domains can be calculated using finite difference methods as applied earlier by Zientara and Freed.[6] The spatial integral of the probability distribution can be related directly to a dimensionless mean lifetime, τ^*, as follows. One first Laplace transforms $P(\mathbf{r},t)$

$$\hat{P}(\mathbf{r},\sigma) = \int_0^\infty e^{-\sigma t'} P(\mathbf{r},t')\, dt' \quad (2a)$$

then we obtain

$$P(\sigma) = \int \hat{P}(\mathbf{r},\sigma)\, d\mathbf{r} \quad (2b)$$

which then yields

$$\tau^* \equiv P(\sigma)/[1 - \sigma P(\sigma)] \quad (2c)$$

where $t' = tD/d^2$ and $\sigma P(\sigma)$ is the probability the domains have not coalesced irreversibly for given σ. The distance of closest approach of the domains is $d = r_a + r_b$, with r_a and r_b the domain radii. (The constant D is discussed below.) For $\sigma \ll 1$, eq 2c yields a σ-independent τ^* value, consistent with the first passage time, i.e., single mode, approximation.

In the absence of interdomain forces, i.e., $U(y) = 0$, the integral formulas of Szabo[3] may be solved exactly for τ^* even with the spatially dependent diffusion coefficient, $D(r) = kT[6\pi\eta d]^{-1}\,[1 - 3d/4r]$, that arises from Oseen's tensor. The method of I enables us to extend this hydrodynamic treatment in the presence of interdomain forces.

Using the general form of the Smoluchowski equation, eq 1, which retains the full properties of the diffusion tensor $\boldsymbol{D}$, we can include the effects of hydrodynamic drag in our calculation. A hydrodynamic treatment of the motion of solute particles includes the consideration of either a slip, stick, or mixed boundary condition at the surface of an impenetrable sphere considered to be moving in an imcompressible fluid which is at rest at infinity.[7] The motion of the solute particles sets up a velocity gradient in the surrounding fluid medium so as to oppose their relative diffusion, and this velocity gradient does depend on the boundary conditions between solute and solvent medium. As in the analysis of diffusion-controlled reactions by Deutch and Felderhof,[8] we will study the hydrodynamic effects on the dynamics of our system by the use of a spatially dependent diffusion tensor

$$\boldsymbol{D}(\mathbf{r}) = D\boldsymbol{I} - 2(k_B T)\boldsymbol{T}(\mathbf{r}) \quad (3a)$$

where Oseen's tensor is introduced

$$\boldsymbol{T}(\mathbf{r}) = (8\pi\eta r)^{-1}[\boldsymbol{I} + \mathbf{rr}(r^{-2})] \quad (3b)$$

Here $D = D_a + D_b$ is the relative diffusion coefficient of unconnected domain centers at infinite separation, which is equal to the sum of their individual Stokes–Einstein values assuming stick boundary conditions at the domain surfaces.[5] η is the solvent viscosity, k_B is the Boltzmann constant, and T is the absolute temperature.

Earlier studies[8,9] of diffusion-controlled reaction dynamics in infinite spatial domains have discussed the adequacy of Oseen's tensor as an approximation to the general Stokes' tensor. Also, others[10] have studied the appropriateness of a slip rather than stick boundary condition in an analysis of macromolecular diffusion and a hydrodynamic description which accounts for the structural nature of protein subunits,[11-13] which are idealized as impenetrable hard spheres in the derivation of eq 3, yet are known to be flexing structures, in some cases penetrable by solvent molecules. After considering these analyses,[8-15] we have employed Oseen's tensor with stick boundary conditions; however, we recognize that these assumptions can overemphasize the effect of the hydrodynamic interaction[10] by a factor of $\sim$1–1.5.

In I and this work we explain the diffusion–reaction approach to domain coalescence through the motion of two spherical domains which are assumed to be connected by a flexible, noninteracting chain. This simplifying assumption neglects the various dynamical (including excluded volume) and electrostatic contributions to domain motion due to the intervening chain and solvent–chain interactions.

To include chain effects in segmental motion without direct modeling of chain dynamics, one may utilize the approximation of an "internal viscosity"[16] applicable to chain elements. An internal viscosity is employed to describe the motion of a particular chain element independent of all individual intrachain interactions. The concept of an internal viscosity was used recently to qualitatively explain fluorescence decay experimental data by Haas et al.[17] Their experimental observations are also supported by the polymer chain molecular dynamics simulations of Gottlib et al.[18] The internal viscosity, η_{int}, is taken to vary as $\eta_{int} = A + B\eta_{solv}$ where η_{solv} is the solvent viscosity and A and B are functions of temperature, ionic strength, and molecular properties of the chain and solvent. The effects of η_{int} have been considered in this study with reference to the temperature dependence of the mean coalescence lifetime, through an ad hoc modification of η appearing in eq 3b.

Pair Correlation Functions. The use of Oseen's tensor to describe deviations from simple Brownian diffusion is clearly more appropriate for dynamical modeling in the cases of large separation of domains. The short range

(6) G. P. Zientara and J. H. Freed, *J. Phys. Chem.*, **83**, 3333 (1979).
(7) L. D. Landau and E. M. Lifschitz, "Fluid Mechanics", Pergamon Press, London, 1959.
(8) J. M. Deutch and B. U. Felderhof, *J. Chem. Phys.*, **59**, 1669 (1973).
(9) J. B. Pedersen and J. H. Freed, *J. Chem. Phys.*, **62**, 1790 (1975).
(10) (a) P. G. Wolynes and J. M. Deutch, *J. Chem. Phys.*, **65**, 450 (1976); (b) P. G. Wolynes and J. M. Deutch, *J. Chem. Phys.*, **65**, 2030 (1976); (c) O. R. Bauer, J. I. Brauman, and R. Pecora, *J. Am. Chem. Soc.*, **96**, 6840 (1974).
(11) (a) J. A. McCammon, J. M. Deutch, and V. A. Bloomfield, *Biopolymers*, **14**, 2479 (1975); (b) M. Kojima and A. Acrivos, *J. Chem. Phys.*, **74**, 4096 (1981).
(12) (a) P. G. Wolynes and J. A. McCammon, *Macromolecules*, **10**, 86 (1977); (b) J. A. McCammon, J. M. Deutch, and B. U. Felderhof, *Biopolymers*, **14**, 2613 (1975).
(13) F. W. Wiegel, "Fluid Flow Through Porous Macromolecular Systems", Springer-Verlag, Berlin, 1980.
(14) D. L. Ermak and J. A. McCammon, *J. Chem Phys.*, **69**, 1352 (1978).
(15) L.-P. Hwang, *J. Chem. Phys.*, **73**, 183 (1980).
(16) (a) A. Peterlin, *Polym. Lett.*, **10**, 101 (1972); (b) R. Cerf, *Chem. Phys. Lett.*, **22**, 613 (1973).
(17) E. Haas, E. Katchalski-Katir, and I. Z. Steinberg, *Biopolymers*, **17**, 11 (1978).
(18) Y. Y. Gotlib, N. K. Balabaev, A. A. Darinskii, and I. M. Neelov, *Macromolecules*, **13**, 602 (1980).

dynamical characteristics of two reacting particles in solution are included employing a reactant pair correlation function which, theoretically, contains statistical information about all solvent–reactant interactions, solvent–solvent interactions, and reactant and solvent molecular structure that will possibly moderate ideal Brownian dynamics.[9,15,19,20]

We have shown in I that the pair correlation function is related to an effective interdomain potential of interaction. The extreme importance of solvation effects in hydrophobic bonding[21,22] necessitates the incorporation of either an interaction potential or pair correlation function in modeling. In I we chose an approximate radially dependent gaussian form of the domain pair mean potential energy due to solvent–domain interactions. To a first approximation this simulated a single solvent shell or solvent cage barrier to diffusion with facilitated motion upon penetration of the solvent cage (see also ref 23).

Within our approach, we assume spherical hydrodynamic qualities of globular domains whose equilibrium properties are sufficiently described through the use of a single radial pair correlation function.[24] This assumption will not be valid when considering proteins in solutions containing denaturing solutes at concentrations which may appreciably alter the domain structure, or at very high temperatures. Within the bounds of the assumption of spherically symmetric domain properties, information regarding the solvation of macromolecules can be extracted from published studies[25-29] of solutes in water and applied to protein domains existing during intermediate protein folding stages.

In this study we employ a model domain pair correlation function in the Smoluchowski equation. The domain pair correlation function written in terms of y, the dimensionless radial domain separation, is $g(y)$ (cf. I), which is related to the dimensionless interdomain potential, $U_m(y) = U_m(r)/kT$, by

$$g(y) = \exp[-U_m(y)] \tag{4a}$$

which can be rewritten as

$$g(y) = g'(y) \exp[-U(y)] \tag{4b}$$

where $g'(y)$ represents the effects on the pair correlation function from domain–solvent and solvent–solvent interactions[25,27] and $U(y)$ is the separable portion of the domain–pair potential (assuming pairwise interactions) used to express the shielded electrostatic interaction between the domains. Since the potential of mean force $U_m(y)$ enters the Smoluchowski equation,[5] we rewrite eq 4 as

$$U_m(y) = -\ln g'(y) + U(y) \tag{5}$$

In order to attempt to model the domain pair correlation function, we will concentrate on the empirical form given by the damped oscillatory function

$$g'(y) \simeq 1 + g_0 \cos[\lambda_0(y-1)] \exp[-\lambda_1(y-1)] \quad \text{for } 1 < y < y_N \tag{6a}$$

with

$$g'(y) = 0 \qquad \text{if } y < 1 \text{ or } y > y_N \tag{6b}$$

The boundary conditions of eq 6b are a restatement of the domain hard-sphere assumption[5] and the extent of the finite spatial domain. Since protein domains are not uniformly hydrophobic, their interactions with the solvent will be nonneglible. Therefore, $g'(y)$ does not exactly represent the pair correlation arising solely from repulsive interactions, $g^{(0)}(y)$, as in the theory of Pratt and Chandler,[27] yet the approximation is consistent within our approach which considers an orientational average of reactivity or hydrophobicity. Thus, the hydrophobic patches on the surface of a domain that eventually will compose the reactive site in coalescence will necessarily have a solvation character closely resembling the results of the recent computational studies.[25,27] An alternate description of solvation effects on the coalescence process would be necessary if it were completely dominated by the interactions of ionizable groups.

We can relate the thermodynamic quantities discussed in I to the modeling parameters using eq 5 and 6. First we have the coalescence energy[5]

$$U_c \equiv U_m(1) = -\ln [1 + g_0] + U(1) \tag{7a}$$

and next the magnitude of the activation barrier encountered prior to domain contact

$$U_{act} \equiv \max\{U_m(y)\} = U_m(y_H) \quad 1 \lesssim y \lesssim y_N \tag{7b}$$

U_c is equal to the difference in the standard molar Gibbs free energies of coalesced and uncoalesced domains through eq 50–52 of I. Explicitly, U_{act} is the activation energy for the primary hydration shell (located at $(r-d) \simeq 1.4$ Å) penetration process while $U_{act} - U_c$ is the activation energy of domain dissociation.

The radial distance from a domain center to the primary solvation shell, y_H, is just the location of the global minimum in $g(y)$ and is a constraint on the choice of the modeling parameters λ_0 and λ_1. Likewise, calculated spatial correlations for hydrophobic spheres in water damp significantly beyond a distance equal to ~2–3 times the diameter of a water molecule. This limits the range of suitable choices of λ_1 (with λ_1^{-1} playing the role of a correlation length). Also, the location of the second maximum in $g(y)$ farthest from $y = 1$ is strongly dependent on the choice of λ_0 and λ_1. For the calculations of section IIIB we have used these constraints to determine the parameters g_0, λ_0, and λ_1. The decay of spatial correlations by $(r-d) \approx 1.4$ Å then requires $\lambda_0 \approx 15$. This produces a second maximum in $g(y)$ at separation $(r-d) \approx 3$ Å as desired. We have also studied the case where the minimum of $g(y)$ occurs at a greater separation, $(r-d) \approx 2.5$ Å, because of the uncertainty in values to be used when the spatial coordinates of domain structures have been averaged over orientations. Equation 7a was used to set the value of g_0 based on the coalescence energy studied. The activation energy, U_{act}, is then regarded as a function of g_0, λ_0, and λ_1.

(19) (a) S. H. Northrup and J. T. Hynes, *J. Chem. Phys.*, **71**, 871, 884 (1979); (b) A. I. Burshtein and B. I. Yakobson, *Int. J. Chem. Kinet.*, **12**, 261 (1980).
(20) L.-P. Hwang and J. H. Freed, *J. Chem. Phys.*, **63**, 4017 (1975).
(21) (a) Y. Paterson, G. Nemethy, and H. A. Scheraga, *Ann. N.Y. Acad. Sci.*, **367**, 132 (1981); (b) G. Nemethy, W. J. Peer, and H. A. Scheraga, *Ann. Rev. Biophys. Bioeng.*, in press. (c) R. Wolfenden, L. Andersson, P. M. Cullis, and C. C. B. Southgate, *Biochemistry*, **20**, 849 (1981); (d) H. A. Scheraga, *Acc. Chem. Res.*, **12**, 7 (1979).
(22) G. Nemethy and H. A. Scheraga, *J. Phys. Chem.*, **66**, 1773 (1962). See also the discussion and references cited in ref 5.
(23) E. Clementi, "Computational Aspects for Large Chemical Systems", Springer-Verlag, Berlin, **1980**, p 91.
(24) It is significant to consider the error introduced by ignoring the detailed spatial distribution of the constituent atoms in a domain when describing domain equilibrium properties using a pair correlation function written in terms of a single internal coordinate. The severity of this approximation is realized when considering orientational dependence of domain hydrophobic, hydrophilic, and electrostatic properties.
(25) C. Pangali, M. Rao, and B. J. Berne, *J. Chem. Phys.*, **71**, 2975, 2982 (1979).
(26) J. C. Owicki and H. A. Scheraga, *J. Am. Chem. Soc.*, **99**, 7413 (1977).
(27) L. R. Pratt and D. Chandler, *J. Chem. Phys.*, **67**, 3683 (1977).
(28) A. Geiger, *Ber. Bunsenges. Phys. Chem.* **85**, 52 (1981).
(29) G. Corongiu and E. Clementi, *Biopolymers*, **20**, 551 (1981).

Application to Experimental Observations. The use of a pair correlation function to explicitly include solvent effects in diffusion–reaction models permits the numerical study of both domain association (i.e., coalescence) and dissociation processes. This follows from the application of the standard treatment of kinetics of reactions in liquids[30] to our consideration of domain coalescence. Phenomenologically, the overall observed rate of formation of a folded protein can be described by considering the mechanism

$$\ldots. \rightleftharpoons \text{domain(A)} + \text{domain(B)} \underset{k_r}{\overset{k_f}{\rightleftharpoons}}$$

$$\text{(AB)domain-pair} \underset{k'}{\overset{k}{\rightleftharpoons}} \ldots.$$

where nucleation steps form the spatially separated domains, prior to the coalescence step. Following coalescence, further folding steps add to the structure of a coalesced domain-pair till final formation of the native protein.

For $k \gg k'$, this simple picture allows us to relate the calculated coalescence lifetime to the kinetic parameters[30]

$$[\tau^* d^2/D]^{-1} = \tau^{-1} = k_f/(1 + k_r/k) \tag{8}$$

where τ has the units of seconds and k_f and k_r are the specific rate constants of domain association and dissociation, respectively. Also, $k \equiv \kappa\Delta_I D/d^2$ is the rate constant describing the depletion of domain pairs in contact, so its value is an adjustable parameter in our calculations from which we consider the time dependence of the coalescence step only. Once the physical quantities that characterize the domain-pair system have been specified and inserted in the model, the predicted values for k_f and k_r can be determined numerically by two calculations. Using the two limiting cases of eq 8, we obtain

$$\tau^{-1} \simeq k_f \qquad \text{for } k \gg 1 \tag{9a}$$

and

$$\tau^{-1} \simeq (k_f/k_r)k \qquad \text{for } k \ll 1 \tag{9b}$$

It is important to note that since few experimental protein studies conclusively distinguish *both* the kinetic and structural features of folding intermediates, the assignment of kinetic constants to a particular folding step, whether a fast step or slow step, is often based only on qualitative arguments. Thus, assignment of experimentally measured reaction rates to domain association and dissociation is most frequently conjecture. Yet, the mechanism of the rate-limiting step in protein folding remains particularly important in protein studies. There exists no clear evidence that domain coalescence is the event which generally constitutes the slowest step in protein folding. For example, in an investigation of ribonuclease A folding in solvents of varying composition, Tsong and Baldwin[31,32] did not observe changes in the rate of the slow step of folding, as would be predicted from a mechanism described by diffusion-controlled domain coalescence. The ionic strength and temperature dependence of folding rates from other published experimental works are, however, correlated with the predictions of our model calculations in section IV.

In the limit that folding steps prior to and following coalescence occur on a shorter time scale than coalescence,

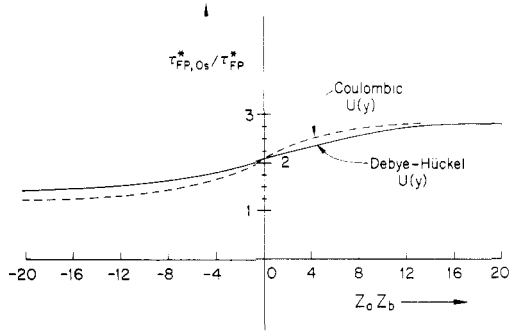

Figure 1. $\tau^*_{FP,Os}/\tau^*_{FP}$, the ratio of the mean coalescence lifetime including hydrodynamic effects and the nonhydrodynamic value, vs. $Z_a Z_b$, the product of the domains' electronic charges. Input includes $\kappa = 5 \times 10^5$, $y_N = 11$, $r_a = r_b$, $\Delta_I = 0.01$, $N = 100$, and an isotropic uniform initial condition. Also, the protein is assumed to be in a 0.15 M univalent salt solution, $d = 10$ Å, $\epsilon = 80$, and $T = 293$ K, so $\kappa_{DH}d = 1.272$.

other relevant quantities can be obtained from the model. Equation 9 can be related to protein denaturation or melting curve data through the percent of denatured protein

$$P(T) = \frac{1}{1 + K(T)} \times 100 \tag{10}$$

where $K(T) = k_f/k_r$ is the ratio of native to denatured protein concentrations at equilibrium.

Numerical Considerations. The computational details of applying Oseen's tensor within the domain coalescence algorithm of I concern the use of the modified finite difference transition matrix, $\boldsymbol{W}$, whose elements have been derived previously by Pedersen and Freed[9] and Hwang[15] and are amended as in I due to our use of an outer reflecting wall boundary condition, which mathematically imposes the finite extent of the accessible diffusive range of the domains.

It is an assumption of this work that the introduction of hydrodynamic interactions and the use of model pair correlation functions still permits the approximation of the mean coalescence lifetime arising from a single exponential decay process.[1,3,5] Each calculation of τ^* by our method involves a single matrix inversion readily accomplished on a small core computer taking advantage of the banded structure of the transition matrix (cf. eq 26–28 of I). Unlike I, the results discussed in this paper have been calculated assuming an isotropic orientational distribution of domains. Further, a uniform orientation dependence of domain interactions and motion is assumed.

Since coalescence lifetime calculations involving a pair correlation function have been found to require smaller finite difference nodal separations (as compared to the values noted in I) for reduction of error, a discretization of 800 (= N) nodes was used in the pair correlation portion of this study. Our tests of convergence showed that the numerical results changed by less than 1% when an additional 100 spatial increments were used, confirming the good level of numerical accuracy. Effects of hydrodynamic corrections in the absence of any interdomain forces (i.e., $U_m(y) = 0$) were calculated and found to correspond to the analytical results of Szabo et al.[3] with negligible (<1%) error.

III. Results of the Extended Model

A. Hydrodynamic Effects with Forces Present. Figure 1 displays the deviation in the mean coalescence lifetime when electrostatic forces and hydrodynamic interactions are present ($\tau^*_{FP,Os}$), as compared to the nonhydrodynamic case (τ^*_{FP}). These results correspond to k_f^{-1} (since $\kappa \gg 1$)

(30) G. G. Hammes, "Principles of Chemical Kinetics", Academic Press, New York, 1978).

(31) T. Y. Tsong and R. L. Baldwin, *Biopolymers*, 17, 1669 (1978).

(32) Tsong and Baldwin (ref 31) studied the viscosity dependence of ribonuclease A folding using sucrose and glycerol viscants. However, the effects of sucrose and glycerol on protein structure stabilization have recently been examined by J. C. Lee and S. N. Timasheff, *J. Biol. Chem.*, **256**, 7193 (1981), and K. Gekko and S. N. Timascheff, *Biochemistry*, **20**, 4667, 4677 (1981), respectively.

TABLE I: Mean Coalescence Lifetimes Including the Effects of a Model Pair Correlation Function and Hydrodynamic Interaction[a]

U_{act}, kcal/mol	$\tau^*_{FP,Os} \times 10^{-2}$			
	$U_c = -1.0$ kcal/mol	$U_c = -1.5$ kcal/mol	$U_c = -2.0$ kcal/mol	$U_c = -2.5$ kcal/mol
2.5	25.4 (26.1)[b]	25.5 (26.2)	24.1 (23.4)	18.6 (22.8)
2.0	16.2 (17.9)	15.5 (17.3)	14.6 (15.5)	13.1 (14.9)
1.5	12.0 (12.8)	11.5 (12.1)	10.7 (11.2)	10.0 (10.4)
1.0	9.4 (9.7)	9.0 (9.1)	8.6 (8.6)	8.2 (7.9)
0.5	7.8 (7.4)	7.5 (6.9)	7.2 (6.5)	7.0 (6.1)
0.1	7.0 (5.9)	6.7 (5.5)	6.6 (5.2)	6.5 (5.0)

[a] Constant input includes $y_N = 11$, $T = 293$ K, $\kappa = 10^{10}$, $\Delta_I = 0.01$, $r_a = r_b$, $N = 800$. The pair correlation function used is given by eq 6 with $(y_H - 1)d \cong 1.4$ Å for $d = 10$ Å. Modeling parameters lie in the ranges $14.5 \leq \lambda_0 \leq 18$ and $9.5 \leq \lambda_1 \leq 38.2$. The value of g_0 for each U_c can be obtained from eq 7a, noting $U(1) = 0$ in this example. An isotropic initial condition with $y_I = 11$ was used for each calculation. No electrostatic forces were included. For the input given, the corresponding force free result is $\tau^*_{Os} = 7.6 \times 10^2$. [b] The results in parentheses were calculated with input identical with that in footnote *a* except that the primary activation barrier was moved outward, $(y_H - 1)d \cong 2.8$ Å for $d = 10$ Å. Modeling parameters then ranged from $4.6 \leq \lambda_0 \leq 11.3$ and $6 \leq \lambda_1 \leq 12$.

and are presented for the cases of Debye–Hückel and Coulombic interactions. The Coulombic case is, of course, the limit of the Debye–Hückel calculations for zero ionic strength. In the range of electrostatic repulsions between domains $0 \lesssim Z_a Z_b \lesssim 20$ it is observed from Figure 1 that hydrodynamic interactions cause an increase by a factor of ~1.5–2.75 in the coalescence lifetimes compared to those predicted in I. Domains experiencing attractive electrostatic forces are found to be generally unaffected by hydrodynamic effects. This corresponds to the results for solute attraction obtained in studies of diffusion in infinite spatial regions.[8,9,15] The results in Figure 1 may be regarded as an upper bound for hydrodynamic effects since we have used stick boundary conditions (see previous section), while the results for τ^*_{FP} give the lower bound. The ratios of Figure 1 can be used to obtain numerical values of $\tau^*_{FP,Os}$ by reference to Figure 5 of I.

Deutch and Felderhof[8] observed that hydrodynamic effects become most significant in the case of equal reactant size, causing a decrease in the reaction rate by a factor of ~1–2 depending on reactant electrostatic charge. Therefore, in this study we have restricted our calculations to the case $r_a = r_b \equiv d/2$, where r_a and r_b are the domain pair radii. The importance of hydrodynamic terms in diffusive dynamics including Debye–Hückel electrostatic reactant interactions has also been studied numerically by Pedersen and Freed[9] and Hwang,[15] who found similar decreases in predicted reaction rates.

Our numerical studies show the insensitivity of τ^*_{FP} to hydrodynamic interactions in the slow reaction limit that may also be seen from Szabo's first-passage time approach.[3] In the diffusion-controlled limit Szabo's formulas assert the importance of hydrodynamic corrections and interdomain interactions, since τ^* is highly dependent on the reactant dynamics, also in agreement with our results.

B. Model Domain Pair Correlation Function. Table I contains results for coalescence lifetimes obtained when a model pair correlation function and hydrodynamic effects are included. The values in Table I were obtained for the $\kappa \to \infty$ limit where $\tau^*_{FP,Os} = k_f^{-1}$ (cf. eq 8 and 9a). As expected, the mean coalescence lifetimes reflect the primary activation barrier height, but the rate of coalescence assumes a partial diffusion-controlled character. In the

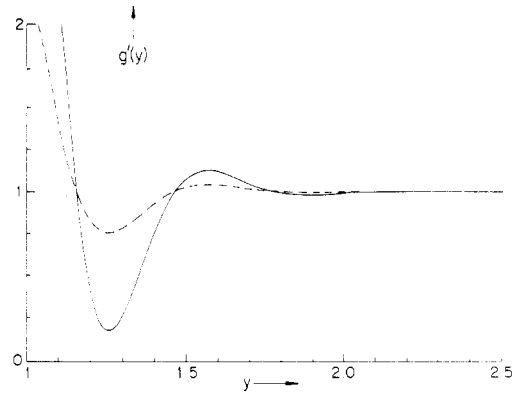

Figure 2. $g'(y)$, the model pair correlation function vs. interdomain separation, y. The solid curve corresponds to a case in which $U_c = -1$ kcal/mol and $U_{act} = 1$ kcal/mol, modeled with input $g_0 = 4.6$, $\lambda_0 = 10$ and $\lambda_1 = 6$. The broken curve corresponds to a case in which $U_c = -0.5$ kcal/mol and $U_{act} = 0.2$ kcal/mol, modeled with input $g_0 = 1.4$, $\lambda_0 = 10$, and $\lambda_1 = 6$. The location of the primary activation barrier is $(y_H - 1)d \simeq 2.5$ Å as shown, if $d = 10$ Å.

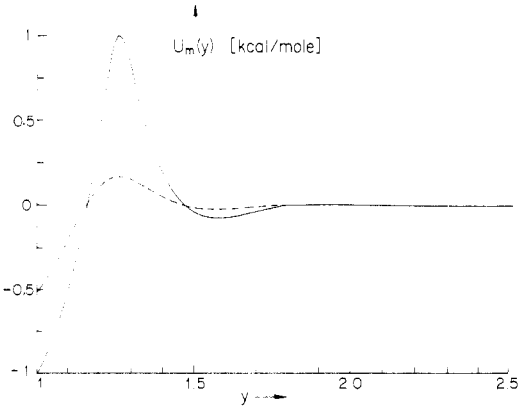

Figure 3. $U_m(y)$, the domain–domain potential of mean force vs. interdomain separation, y. Both the solid and broken curves refer to the respective curves of $g(y)$ seen in Figure 2: (solid curve) $U_c = -1$ kcal/mol and $U_{act} = 0.2$ kcal/mol; (broken curve) $U_c = -0.5$ kcal/mol and $U_{act} = 0.2$kcal/mol.

range of U_{act} between 1 and 2 kcal/mol, $\tau^*_{FP,Os}$ varies approximately linearly with U_{act} for constant U_c. In contrast, $\tau^*_{FP,Os}$ is slowly varying as U_c is progressively made large and negative, indicating that the effective domain attraction experienced after penetration of the hydration shell does not significantly increase the forward rate of coalescence, although it is important.

Figure 2 shows the form of $g'(y)$ used in this study, with the corresponding potential of mean force, $U_m(y)$, illustrated in Figure 3. Recall that the pair correlation function includes the effects of solvent-solvent and solvent–domain interactions. The thermodynamically relevant quantities from eq 7, U_c and U_{act}, therefore are measures of the solvent structure surrounding a hydrophobic solute or, here, a domain with an averaged hydrophobic character. Values for the thermodynamic quantities describing the formation of hydrophobic bonds between amino acid side chains have been given by Nemethy and Scheraga[22] and others.[21] Values of molar $\Delta G°$ for amino acids reported for 25 °C range from –0.3 to –1.6 kcal. The total hydrophobic bonding energy of domain coalescence, U_c, is then a sum of the contributions of side chains participating in bonding. The value of U_{act} includes the effects of possible hydrogen bonding between protein segments and water and between individual water molecules in the surrounding hydration shell. Restructuring of the hydrogen bonds that exist in the solvent cage sur-

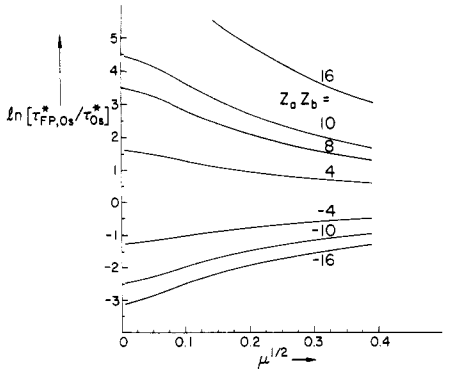

Figure 4. Plots of ln $[\tau^*_{FP,Os}/\tau^*_{Os}]$ vs. $\mu^{1/2}$ for different values of the product of domain charges. $\tau^*_{FP,Os}/\tau^*_{Os}$ is the ratio of the coalescence lifetime including the effects of Debye–Hückel electrostatic interactions to that obtained for uncharged domains. $\mu^{1/2}$ is displayed in units of $M^{1/2}$. Input includes $T = 310$ K, $d = 10$ Å, $\epsilon = 80$, $\kappa = 10^{10}$, $r_a = r_b$, $N = 100$, $\Delta_I = 0.01$, and an isotropic, uniform initial condition. $\tau^*_{Os}(\kappa \to \infty) = 6.7 \times 10^2$ is the force free result.

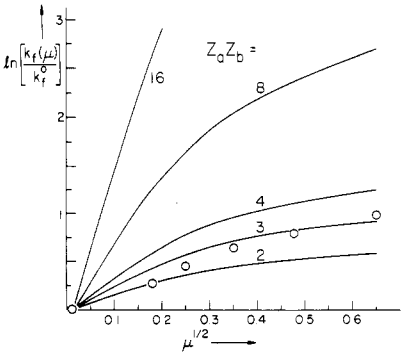

Figure 5. Plots of ln $[k_f(\mu)/k_f^\circ]$ vs. $\mu^{1/2}$ for different positive values of Z_aZ_b. k_f° is the predicted rate constant for coalescence at $\mu = 10^{-4}$ M, specific to the value of Z_aZ_b. Circles are temperature-jump data of Pohl (ref 40) for the ionic strength (LiCl) depencence of trypsin folding at pH 2.2. Numerical results were calculated using the input $\kappa = 10^6$, $N = 100$, $y_N = 11$, $d = 10$ Å, $T = 37$ °C, $\Delta_I = 0.01$, $r_a = r_b$, and a uniform isotropic condition. Hydrodynamic effects are included in these results.

rounding the domains can produce a marked variation in U_{act}. Though the rate of domain coalescence and the rate of dissociation are functions of $U_m(y)$, the rate of dissociation exhibits the stronger dependence with $k_r \propto \exp[-(U_{act} - U_c)]$. (Note: U_{act} and U_c are dimensionless here.)

Experimental studies of protein denaturation commonly take advantage of solvent structure perturbation techniques. An important solvent effect of a denaturant is the disruption or reformation of the hydrogen bonding networks in water,[33] which influences the clathrate structure around protein side chains.[34] Denaturants generally reduce[33,34] the magnitude of ΔG° of folding (thus reducing U_c in our analysis), although exceptions exist in certain concentration ranges and temperatures. Pohl[35] noted in a study of trypsin folding that alcohol denaturant effects included a decrease in the apparent activating energy governing renaturation (i.e., U_{act}). Additional solution components that hydrogen bond with protein segments can also sterically interfere with folding events, a different mechanism than solvent structure perturbation.

The sensitivity of the rate constant of coalescence to the hydration shell parameters is shown in the results of Table I, through the change in $\tau^*_{FP,Os}$ as the magnitudes of both U_{act} and U_c vary. Though the dependence of $\tau^*_{FP,Os}$ on U_{act} and U_c differs, a net decrease in $\tau^*_{FP,Os}$ is observed as the magnitudes of both U_c and U_{act} decrease. In cases of $|U_c| > U_{act}$ and $U_{act} < 1$ kcal/mol the predicted lifetime is actually shorter than the result in the absence of any activation barrier, where $U_{act} = U_c = 0$ (cf. footnote *a*, Table I). The results of Table I demonstrate that $\tau^*_{FP,Os}$ is dependent on the energetics of coalescence such that 0.5–1.0 kcal/mol variations in the thermodynamic quantities associated with hydrophobic bonding, U_c and U_{act}, would produce experimentally observable variations in the time dependence of coalescence. From the data of ref 21 and 22 we note that a variation in U_c of 0.5–1.0 kcal/mol could be attributed to the formation or lack of formation of as few as ~1–3 hydrophobic bonds between amino acid side chains.

IV. Comparison with Experimental Results

A. Dependence of k_f on Ionic Strength. In Figure 4 we exhibit the ionic strength (i.e., μ) dependence of $\tau^*_{FP,Os}$ for several cases of charged domains including both electrostatic and hydrodynamic interactions. We have used τ^*_{Os} to represent the coalescence lifetime for uncharged domains including Oseen's tensor hydrodynamic interactions. Computed in the limit $\kappa \to \infty$, our calculations yield values of $\tau^*_{FP,Os} = k_f^{-1}$. The results for $\mu \gtrsim 0.01$ reveal an ionic strength variation similar to that of freely diffusing charged reactants in solution,[30] i.e., $\ln [k_f/k_f(\mu = 0)] \propto Z_aZ_b\kappa_{DH}d/(1 + \kappa_{DH}d)$, with the inverse of the Debye length $\kappa_{DH} \propto \mu^{1/2}$. All results in Figures 1 and 4 were obtained within the range of validity of Debye–Hückel ionic strength,[36] i.e., $\kappa_{DH}d \lesssim 3$. In our calculations we assumed that the dielectric constant of water is independent of the ionic strength. This is known to be a good approximation[37,38] even for the maximum mole fraction of ions considered $\simeq 0.02$) which corresponds to $\mu = 0.4$ M to $\mu = 0.15$ M.

For charged domains with $|Z_aZ_b| \gtrsim 10$, Figure 4 shows a strong ionic strength dependence of $\tau^*_{FP,Os}$ displaying approximately an order of magnitude variation as μ decreases from 0.15 M to 0.001 M. A weaker ionic strength dependence is obtained for domains where the magnitude of the net charge product is $\lesssim 10$.

Strongly acidic (or basic) experimental conditions will generally protonate (or deprotonate) all solvent-exposed ionizable protein groups. In both these pH limits domains will typically carry like charges and Z_aZ_b will be positive. Predictions for the ionic strength dependence of the coalescence rate constant, k_f, are shown in Figure 5 for several values of $Z_aZ_b > 0$. The variation in $k_f(\mu)$ is shown relative to the low ionic strength ($\mu = 10^{-4}$ M) limiting value. The predicted rate of coalescence increases significantly, for fixed Z_aZ_b, reflecting the effect of ionic shielding of the repelling domains. Temperature-jump data of trypsin folding from Pohl[39] recorded under strongly acid conditions are compared to the predictions in Figure 5. However, the trypsin results of Pohl refer to a single rate-limiting folding step whose mechanism has not yet been determined experimentally.

A complication in the analysis of experimental data is encountered when attempting to use the results shown in Figure 4 for predictive purposes due to the variation of protein charge with the solvent ionic strength.[40] Hammes

(33) F. Franks and D. Eagland, *CRC Crit. Rev. Biochem.*, 3, 165 (1975).
(34) J. F. Brandts, *J. Am. Chem. Soc.*, 86, 4291 (1964); 89, 4826 (1967).
(35) F. M. Pohl, *Eur. J. Biochem.*, 7, 146 (1968).
(36) G. Bell, S. Levine, and L. McCartney, *J. Colloid Interface Sci.*, 33, 335 (1970).
(37) H. S. Harned and B. B. Owen, "The Physical Chemistry of Electrolyte Solutions", 3rd ed., Reinhold, New York, 1958.
(38) (a) G. Scatchard, *Chem. Rev.*, 19, 309 (1936); (b) J. Wyman, *J. Am. Chem. Soc.*, 58, 1482 (1936).
(39) F. M. Pohl, *FEBS Lett.*, 3, 60 (1969).

and Alberty[41] hve discussed the use of an average protein charge to simplify this problem, recognizing that the average value represents an approximation appropriate over a small range of both pH and ionic strength. The results of our calculations can be used to analyze experimental observations if the protein charge (i.e., value of Z_aZ_b) is changed as μ is changed. We first note that each curve in Figure 4 was calculated for a specific value of Z_aZ_b. As μ is increased, the mean coalescence time for domains with fixed charge will increase (for $Z_aZ_b < 0$) or decrease (for $Z_aZ_b > 0$), to the limit $\tau^*_{FP,Os}(\mu \gg 1\ M) = \tau^*_{Os}$. The *opposite* variation of $\tau^*_{FP,Os}$ with μ can be predicted, however, in cases where the magnitude of Z_aZ_b increases with μ. An example of this effect is demonstrated by comparing the values of $\tau^*_{FP,Os}(Z_aZ_b = 4, \mu = 0.1\ M)$ and $\tau^*_{FP,Os}(Z_aZ_b = 16, \mu = 0.4\ M)$ from Figure 4. Therefore, it is possible to predict a constancy in τ or k_f with ionic strength under certain conditions which, however, are in the regime where the time dependence of domain coalescence is strongly affected by electrostatic interactions. Unfortunately, a folding step proceeding through an entirely different mechanism can also display insensitivity to ionic strength variation.

Several processes can account for the variation in domain charges as μ is increased: (1) the binding of ions by a protein[40] and (2) intradomain conformational changes which expose or "bury" charged groups, or allow side chains to orient forming salt bridges. As a further complication, a variation in τ with μ can also be produced by the effects of ions in solution on chain segment motion. The moderation of intrachain electrostatic interactions due to ionic shielding can: (1) increase the domains' available diffusive space, which alone would tend to lengthen the mean coalescence lifetime (cf. eq 45 of I, where $\tau^* \propto y_N^3$), and (2) change the chain segment diffusivity described through the ionic strength dependence of an apparent internal viscosity.

Because of these analytical difficulties, we conclude that the information obtained in ionic strength dependent measurements of protein folding times need not always disclose the diffusive nature of folding steps nor alone reveal unambiguously the electrostatic effects on folding.

B. Dependence of k_f on Temperature. Predictions. The temperature dependence of the mean coalescence lifetime τ ($= \tau^* d^2/D$) enters implicitly through the diffusion coefficient (via $\eta_{int} = A + B\eta_{H_2O}$), the dielectric constant of water $\epsilon(T)$, and the pair correlation function $g(y)$. The dependence of η_{H_2O}[42] and ϵ[43] on temperature has been taken from published formulas based on experimental data. At present, the temperature variation of $A(T)$ and $B(T)$ is not adequately understood,[16] complicating any attempt to describe $\eta_{int}(T)$ rigorously. Similarly, an empirical description of the change of $g(y)$ is lacking. However, the graphical results of Pratt and Chandler[27] for free nonpolar particles in water reveal a variation in $g(y)$ as temperature increases from 4 °C to 50 °C. This change corresponds to an increase in the primary activation barrier at high temperatures as water takes on the characteristics of a hard-sphere solvent. A much weaker increase in the magnitude of U_c is noted over this temperature range.

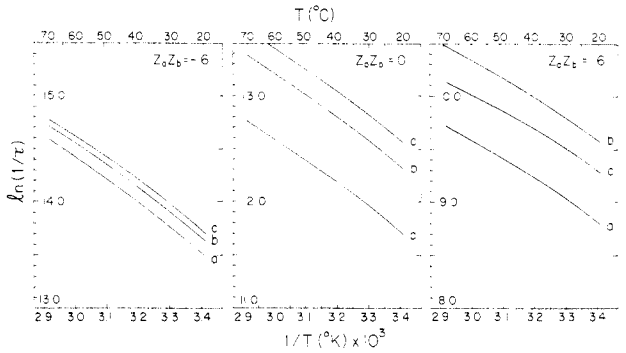

Figure 6. Plots of ln $(1/\tau)$, the logarithm of the coalescence rate constant, vs. inverse temperature for $Z_aZ_b = -16, 0, 16$, as shown. Results correspond to (curve a) $U_c = -1.7kT$, $U_{act} = 3.4kT$, $y_H = 1.25$; (curve b) $U_c = -1.7kT$, $U_{act} = 1.7kT$, $y_H = 1.25$; and (curve c) no correlation function employed. Other modeling input includes $N = 800$, $y_N = 11$, $y_I = 11$, $\kappa = 10^6$, $\Delta_I = 0.01$, and an isotropic initial condition. Included are hydrodynamic effects and Debye–Hückel electrostatic interactions assuming $\mu = 0.15$ M, $r_a = r_b$, and $d = 10$ Å.

In Figure 6 we show the predicted Arrhenius plots of ln $(1/\tau)$ [or ln k_f] for a negative, zero, and positive value of Z_aZ_b. In order to obtain these results it was necessary to make the simplifying assumptions for the reasons noted above: (1) $\eta_{int} \approx \eta_{H_2O}$, and (2) $U_m(r)/kT = f(r)$. Curves a, b, and c represent cases modeled with activation energy barriers of (a) $3.4kT$, (b) $1.7kT$, and (c) no barrier. These results then form the bounds on results that would be obtained employing $U_m(r)/kT = f(r,T)$. This more realistic use of a temperature dependent $U_m(r)/kT$ is discussed below. These approximate results, however, simplify the discussion of the effects of bulk solvent properties on coalescence. From Figure 6 we observe that the various fixed Z_aZ_b cases predict approximately an inverse temperature dependence of the log of the forward coalescence rate constant, common to an Arrhenius description. The slope of a linear fit of the results in Figure 6 yields an apparent activation energy of ~4.5 kcal/mol in all cases of Z_aZ_b, although *no* activation barrier of this magnitude was included in the model, as is evidenced most clearly from the results obtained without use of a pair correlation function (curves c in Figure 6). The temperature dependence of the predictions therefore is a measure of the viscous and energetic aspects of the diffusive dynamics governed particularly by solvent properties. In our computations we have concentrated on the range of temperature from 20 to 70 °C, common to thermal denaturation–renaturation experiments. As the temperature is increased from 20 to 70 °C the dielectric constant of water decreases[43] ~20%, and the viscosity of water decreases[42] ~60%. The change in the dielectric properties of water is effective in slightly increasing the electrostatic force of repulsion between domains with like charges. In I (cf. Figure 5 of I) computed predictions for τ^*_{FP} or k_f revealed a significant dependence on electrostatic forces, particularly for charged domains where $Z_aZ_b > 4$. From the results in I for $Z_aZ_b > 4$ we conclude that interdomain repulsion is able to measurably reduce k_f compared to the cases of uncharged or oppositely charge domains. Hydrodynamic interactions also enchance the dependence of k_f on electrostatic interactions for cases of positive Z_aZ_b, as seen in Figure 1.

The corrections due to the change in the primary activation energy barrier of the mean domain interaction at higher temperatures[27] can be determined qualitatively from Figure 6. If, for example, the primary activation barrier energy approximately doubled as the temperature

(40) (a) C. Tanford, "Physical Chemistry of Macromolecules", Wiley, New York, 1961; (b) J. Steinhardt and J. A. Reynolds, "Multiple Equilibria in Proteins", Academic Press, New York, 1969.
(41) G. G. Hammes and R. A. Alberty, *J. Phys. Chem.*, **62**, 274 (1959).
(42) "Handbook of Chemistry and Physics", R. C. Weast, Ed., 51st ed., Chemical Rubber Co., Cleveland, 1970.
(43) (a) A. A. Maryott and E. R. Smith, NBS Circular 514, Washington, DC, 1951; (b) C. G. Malmberg and A. A. Maryott, *J. Res. Natl. Bur. Stand.*, **56**, 1 (1956).

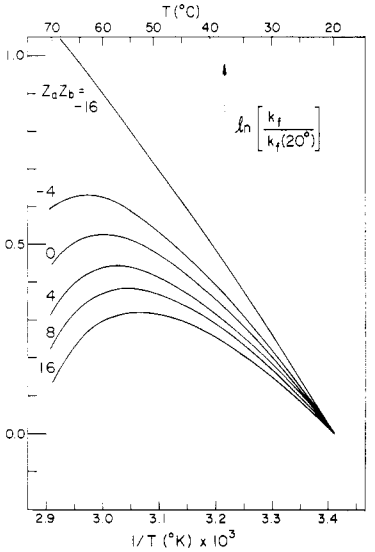

Figure 7. Plots of ln $[k_f/k_f(20\ °C)]$ vs. inverse temperature for different values of Z_aZ_b at ionic strength μ = 0.15 M. Note, $k_f(20\ °C)$, the coalescence rate constant at 20 °C, differs with μ and Z_aZ_b. Results were obtained using input N = 800, y_N = 11, y_I = 11, Δ_I = 0.01, $\kappa = 10^6$, d = 10 Å, $r_a = r_b$, and isotropic initial condition with hydrodynamic and Debye–Hückel electrostatic interactions. The model pair correlation function parameters used are g_0 = 4.57, λ_1 = 6.0. λ_0 is allowed to vary linearly with temperature from 10.0 at 20 °C to 11.5 at 70 °C; thus $y_H \simeq 1.25$.

increased from 20 °C, then the predictions of ln k_f would be best approximated by the results in curve b at $T \approx 20$ °C and the results in curve a at higher temperatures. This qualitative argument demonstrates two different effects: (1) for Z_aZ_b negative, i.e., oppositely charged domains, the temperature dependent results would be relatively *insensitive* to short range solvent cage factors; (2) for domains of zero or like charges, $Z_aZ_b \gtrsim 0$, changes in the solvent cage characteristics would emphasize the decrease in k_f at higher temperatures.

Figure 7 shows the relative variation in k_f when we explicitly include the change in the primary activation energy barrier of the mean domain interaction at temperatures above 4 °C. The increase in the barrier energy is based upon the results of Pratt and Chandler[27] for nonpolar (spherical) solute pair correlation functions which vary due to the tendency of water to assume hard-sphere solvent qualities with increasing temperature. Hard-sphere molecules can be more closely packed about the surface of a nonpolar solute compared to the packing of water in a hydrogen bonded clathrate structure. Thus, the exact magnitude and description of the variation of U_{act} is a function of solute (i.e., domain) composition and dimensions. To calculate the results in Figure 7 we have chosen a linear temperature variation in U_{act}, from $1.7kT$ at 20 °C to $3.4kT$ at 70 °C. The weak variation and magnitude of U_{act} are used only to approximately include the changing solvent properties of water. From Figure 7 we observe the temperature-dependent competition between the effects of the reduced viscous forces, and the electrostatic forces and solvation shell barrier variation. This competition is most manifest in cases of large, positive Z_aZ_b, as expected.

An interpretation of the Figure 7 results found using $Z_aZ_b \gtrsim -4$ yields a temperature-dependent apparent activation energy, if on straightforwardly applies an Arrhenius rate constant analysis. Calculated apparent activation energies obtained from these particular results by linearization over small temperature increments range from about +2 kcal/mol (Z_aZ_b = 16, 20 °C $\leq T \leq$ 45 °C) to about −3.5 kcal/mol (Z_aZ_b = 16, 60 °C $\leq T \leq$ 70 °C). The predictions of this section therefore reveal clearly that an Arrhenius analysis is inappropriate when applied to the results of such a diffusive process as we have modeled.

The results shown in Figure 7 found using $Z_aZ_b \gtrsim -4$ and μ = 0.15 M indicate a temperature at which there is predicted a maximum coalescence rate within the range 20 °C $\leq T \leq$ 70 °C. Similarly, this maximum rate is predicted for slightly higher values of Z_aZ_b when μ increases, since ionic shielding has diminished domain interactions compared to the example of μ = 0.15 M. For large values of Z_aZ_b and $\mu \to 0$, one approaches the limit where $\partial \ln k_f/\partial(1/T)$ is always negative for 20 °C $\leq T \leq$ 70 °C.

Corrections to the results found in Figures 6 and 7 are necessary due to the internal viscosity approximation utilized, $\eta_{int} \approx \eta_{H_2O}$. The form $\eta_{int} \approx C \exp[U/RT] + B\eta_{H_2O}$ as suggested by Peterlin[16a] was employed in the recalculation of the results in Figure 7. Within this approximation of η_{int}, C, B, and U are constants, independent of temperature and calculated from chain properties. A uniform and temperature-independent reduction in k_f of an order of magnitude resulted from these computations. This result is consistent with the experimental data for a segmental diffusion coefficient obtained by Haas et al.[17]

Experimental Comparison. The predicted temperature dependence of the rate of coalescence can be easily compared to temperature-jump experiment results and results from several other techniques. The temperature-jump technique is most suitable, since it does not depend on the use of additional chemical components to perturb the equilibrium between the folded and unfolded protein states. Therefore, it is a useful kinetic probe of a reaction process such as domain coalescence, which is expected to proceed at a rate that is highly sensitive to many solvent and protein interactions. Due to the complex multistep kinetics of the entire protein folding process, experiments may resolve information about a single kinetically dominant folding step[44-48] or several folding steps.[49,50] The interpretation of these data is nontrivial when one attempts to recreate a folding scenario and to apply findings to a specific folding event. To apply such data to domain association is, then, supported only by qualitative arguments and comparison with model predictions.

The results seen in Figure 7 for $Z_aZ_b \gtrsim -4$ indeed demonstrate the qualitative behavior observed in many protein folding studies.[44-49] The experimental data referred to describe the temperature dependence of a rate constant, k_f^{exp}, of a single folding step. The *predicted* temperature dependence of k_f (the domain coalescence rate constant) for $Z_aZ_b \gtrsim -4$ reveals a marked deviation from an Arrhenius description with a temperature dependent maximum in k_f obtained for intermediate values of Z_aZ_b and a change in the sign of the slope $[\partial \ln k_f/\partial(1/T)]$ at large values of Z_zZ_b. Examples of proteins which exhibit one of these types of temperature dependence are (temperature-jump results unless noted): chymotrypsinogen A[44a] and B,[39] chymotrypsinogen,[44b] α-chymotrypsin,[44b] trypsin,[35] elastase,[44d] ribonuclease A,[44d,45] α-lactalbumin,[46], lysozyme,[47] deoxyribonuclease (difference spectroscopy),[48] and ferricytochrome c.[49] This observed temperature depen-

(44) (a) F. M. Pohl, *FEBS Lett.*, **65**, 293 (1976); (b) F. M. Pohl, *Eur. J. Biochem.*, **4**, 373 (1968); (c) F. M. Pohl, *Angew. Chem.*, **11**, 894 (1972).
(45) P. McPhie, *Biochemistry*, **11**, 879 (1972).
(46) K. Kuwajima and S. Sugai, *Biophys. Chem.*, **8**, 247 (1978).
(47) S.-I. Segawa, Y. Husimi, and A. Wada, *Biopolymers*, **12**, 2521 (1973).
(48) S. B. Zimmerman and N. F. Coleman, *J. Biol. Chem.*, **246**, 309 (1971).
(49) T. Y. Tsong, *Biochemistry*, **12**, 2209 (1973).
(50) H. F. Epstein, A. N. Schechter, R. F. Chen, and C. B. Anfinsen, *J. Mol. Biol.*, **60**, 499 (1971).

dence cannot be adequately explained by standard theories. The results of Pohl in the study of α-chymotrypsin[44b] and trypsin[35] show that the maximum in k_f^{exp} shifts to lower temperatures when folding is studied at lower pH conditions, as expected from our k_f predictions for increasing Z_aZ_b in Figure 7. The identical pH dependent shift in the maximum of k_f^{exp} was observed by McPhie in the study of ribonuclease A. Interestingly, Segawa et al.[47] obtained k_f^{exp} temperature-dependent results in the folding study of lysozyme (with μ = 4.5 M) that correspond qualitatively with our predictions for highly charged domains $Z_aZ_b \gg 0$, where $\partial \ln k_f^{exp}/\partial \ln (1/T) > 0$ for 30 °C $\leq T \leq$ 50 °C.

Thus we see that a common observation, which appears anomalous in the context of an approach based on simple Arrhenius rate constants, can be interpreted by our model results in terms of the temperature dependence of the solvent structure vs. the viscosity. While our model results do not yield quantitative agreement, there is considerable room for improvement of the simple model.

V. Summary

In I we described the diffusive model of protein domain coalescence which forms the basis of the protein folding event that is the focus of the present study.

A reduced variable model of the dynamics and interactions between protein domains and solvent components must, for practical reasons, include numerous approximations and be based upon many assumptions. Our approach assumes that folding events such as nucleation and domain formation have occurred prior to coalescence and that other folding events can take place after coalescence to stabilize a coalesced domain pair and conclude the formation of a native structure of the protein. Therefore, coalescence (i.e., domain association) has been depicted as the elementary reaction step in the multistep formation of correct or abortive intermediates[51] in a multiple-domain protein. In the calculations of this work, spatial and time averages of the discrete conformational and electrostatic properties of the domains have been utilized. We have neglected interactions between ionic or denaturant solution components and the amino acids of the chain connecting domains. These many interactions are specific to each protein and will inevitably cause deviations between experiment and any predictions derived from a simple, generally applicable model. The excluded volume effect due to the finite size of the connecting chain is not explicitly included, yet can be accounted for roughly in our theory through η_{int}. Excluded volume effects will contribute to the decreased diffusivity of the domains relative to free particle values. The temperature dependent variation in the bulk solvent properties of water has been included in the model through $\eta_{H_2O}(T)$ and $\epsilon(T)$.

The Smoluchowski equation solution of domain diffusion and association in I has been extended in this work to include an Oseen's tensor hydrodynamic interaction and a model domain pair correlation function. The Debye–Hückel shielded electrostatic potential and Oseen's tensor hydrodynamic interaction represent approximations valid for the treatment of particles immersed in a continuum fluid. However, as a departure from this level of solvent modeling we have employed a pair correlation function with molecular scale detail to specifically include the domain solvation characteristics that are extremely important in describing hydrophobic bond formation. Hydrodynamic effects were observed to alter model predictions by increasing $\tau^*_{FP,Os}$ for domains experiencing electrostatic repulsion. This case of positive domain charge product, that is $Z_aZ_b \geq 0$, is most applicable to protein systems since ionizable groups contained in both protein domains will be similarly affected by pH and ionic strength conditions. The sensitivity of τ (thus k_f) to the solvent properties of water was examined by the use of a pair correlation function from which a mean interdomain potential can be derived. Variations of the order of ~1 kcal/mol in the energy of activation or coalescence energy were found to predict significant changes in τ.

The effects of the model parameters on τ have been discussed in detail. The predictions of the complete model were compared with experiments. The ionic strength dependence of τ was discussed to illustrate that changes in protein domain charge with ionic strength can lead to apparently anomalous behavior. A simple analysis was presented to show that electrostatic effects on τ must be considered as a function of pH, μ, and Z_aZ_b. Although this conclusion follows readily from Debye–Hückel theory, it is emphasized that in the case of coalescence, a single μ-dependent folding experiment is ambiguous on the details of electrostatic effects.

Finally, the temperature dependence of the coalescence rate was discussed. The rate constant k_f in cases of $Z_aZ_b \gtrsim -4$ was predicted to exhibit a temperature dependence deviating greatly from an Arrhenius description. Within a certain range of Z_aZ_b (related to ionic strength conditions), a temperature dependent maximum in k_f is predicted. This characteristic feature in k_f has been observed in folding experiments on many proteins and has been regarded as an anomaly. Our analysis has clearly and naturally shown that this result is an effect of the temperature-dependent competition between the variation in the domains' diffusivity (through η_{int} and η_{H_2O}) on the one hand and the combination of increased electrostatic interaction and changes in liquid water structure on the other.

It is clear that the stochastic modeling of domain coalescence requires a number of physical factors. That is, the domain diffusion–association process is *not* easily explained either in the simple context of free particle diffusion-controlled kinetics (cf. the basis of ref 31) nor just in chain end diffusion of polymers. Rather, domain coalescence, as our model reveals, relies on the structural properties of liquid water, the presence of ions in solution, protein chain segment motion, electrostatic domain–domain interactions, and domain hydrophobic character. These quantities also exhibit a temperature and composition variation. Most important, our predictions emphasize the cooperativity or competition between these factors in regulating the rate of coalescence. Although the coupling of these factors poses a difficult problem for theoretical analysis, their consideration has been shown to be critical in accurate modeling of domain coalescence. Ultimately, it is hoped that a careful analysis of this single event will aid in the understanding of the dynamics of the entire folding process.

Acknowledgment. J. A. N. wishes to acknowledge the guidance and support provided by Professor H. A. Scheraga.

(51) (a) A. Ikai and C. Tanford, *Nature (London)*, **230**, 100 (1971); (b) L. L. Shen and J. Hermans, Jr., *Biochemistry*, 11, 1836 (1972); (c) O. B. Ptitsyn and A. A. Rashin, *Biophys. Chem.*, 3, 1 (1975); (d) F. E. Cohen, M. J. Sternberg, D. C. Phillips, I. D. Kuntz, and P. A. Kollman, *Nature (London)*, **286**, 632 (1980).